Propagation Losses and Impulse Response of the Indoor Optical Channel: A Simulation Package

Cipriano R. A. T. Lomba Rui T. Valadas
A.M. de Oliveira Duarte
Dept. of Electronics and Telecommunications
University of Aveiro, PORTUGAL

Abstract

In this paper we present a simulation package developed to evaluate and optimize both the channel propagation losses and the multipath dispersion of the indoor optical channel. The simulation package is based on a model of the indoor optical channel which includes the emitter radiation pattern, the channel propagation characteristics and the receiver collecting pattern. We illustrate the use of the simulation package by means of two case studies corresponding to: i) a satellite based cell and ii) a passive reflection based cell. It is seen that optimization of the emitting pattern by tuning the number, orientation and radiation pattern of the LEDs can significantly reduce the worst-case channel losses and increase the channel bandwidth. The channel impulse response changes with the receiver position, therefore, techniques to combat the multipath dispersion have to be used for bit rates higher than a few Mbit/s.

This work is being carried out as part of the ESPRIT.6892 - POWER (Portable Workstation for Education in Europe) project commissioned by the European Community.

1 Introduction

The need and demand to communicate and share software applications, data bases and information in general while keeping mobility have increased very rapidly over the past few years. This growth pushed the development of practical and flexible communication networks. Wireless networks represent a very good alternative to cabled networks for indoor applications. Indoor wireless communication systems can be used in a wide range of applications to provide for portability, user mobility and easy set-up of networking resources.

Indoor wireless systems can use two kinds of carrier to convey the information: radio waves or infrared radiation. The use of a particular technology depends mainly upon the envisaged application and the physical channel characteristics. In this work, we concentrate on indoor communication systems using infrared technology.

Recently, infrared technology based systems have been receiving significant interest because they are easier to implement than radio systems, do not require any licensing, are not affected by electromagnetic noise interference and provide for privacy outside the room premises.

Indoor infrared systems are mainly impaired by three factors: interference from ambient light (sun light and artificial illumination), multipath dispersion (for data rates higher than a few Mbit/s, depending on the room dimensions) and technological limitations of the available optoelectronic devices.

This paper presents a simulation package developed for simulation of the indoor optical channel. The present implementation of the package was designed for two distinct applications: evaluation and optimization of the propagation losses and evaluation and optimization of impulse response. The latter is important for future high bandwidth systems whereas the former is important for all systems, in particular, those being presently considered by the standardisation bodies. A brief discussion of the characteristics of the quasi-diffuse and diffuse propagation modes is given in section 2. The model of the optical channel used in the simulation package is presented and discussed in section 3. Section 4 illustrates the use of the simulation package by means of two case studies. Finally, section 5 presents the main conclusions of the work.

This work is being carried out as part of the ESPRIT.6892 - POWER (Portable Workstation for Education in Europe) project commissioned by the European Community.

2 The Diffuse and Quasi-Diffuse Propagation Modes

The propagation modes of indoor infrared systems have been extensively discussed in the literature [1, 2, 3]. Our main interest is the characterization of the indoor channel under the diffuse and quasi-diffuse propagation modes. In both modes the signal emitted by one station is broadcasted to all the other stations in the room, emitters and receivers have relatively large emitting beams and field-of-views, FOV, respectively. A direct line-of-sight between emitter and receiver is not required.

In the diffuse propagation mode, the emitted radiation is reflected at all room surfaces and the room volume becomes filed with infrared radiation. No orientation of the transceivers is required as the signal radiation arrives at the receiver location from every direction.

In the quasi-diffuse propagation mode, the emitted radiation is reflected at only one surface and all stations must have a direct path to that surface. Usually, the reflecting surface is the room ceiling which must present good reflection characteristics. If the room ceiling does not reflect properly the infrared signals or if one intends to extend the coverage area an active reflector can be used. This active reflector also called *satellite* is mounted at the ceiling. The satellite receives the signal broadcasted by the emitting stations, amplifies and then broadcasts it again. Two variations of the quasi-diffuse mode will be considered:

- Targeted orientation: assumes the user will have to point the optical interface of the transceiver to the satellite or to some specific point at the room ceiling if the system uses passive reflection.
- Natural orientation: assumes that all terminals have a large emitting beam and receiving FOV and are oriented vertically.

3 Model of the Indoor Optical Channel and Simulation Package

This section presents the model of the optical indoor channel used in the simulation package. The model includes the characteristics of the emitted optical beam, the effects of the channel over that beam and the receiver optical collection characteristics.

The main characteristics of the indoor optical channel are now summarized. The power emitted by the source is spread over the room space. The power spreading profile depends directly on the source position, orientation and radiation pattern. The emitted beam incides on the room walls and furniture and is partially reflected according to the reflection coefficients and patterns of the surfaces. The optical power collected at the receiver depends on the receiver position, orientation, FOV and active area. The received signal results from the direct signal (line-of-sight) and multiple-order reflected signals that incide into the detector active area. The signal collected from the multiple-order reflections will result on a signal delay spread or intersymbol interference.

3.1 The Source Model

Indoor infrared communication systems usually use short wavelength (820 - 920 nm) Light Emitting Diodes (LEDs). Following Gfeller [1] the radiant intensity of a LED can be modelled using an extension of the Lambertian law given by

$$E(\phi) = \frac{n+1}{2\pi} P_t \cos^n(\phi) \tag{1}$$

where P_t is the total emitted power, ϕ is the angle with the normal to the LED lens and n is a parameter indicating the beam width and is given by

$$n = -\frac{0.693}{\ln[\cos(HPBW)]} \tag{2}$$

where $HPBW$ is the LED half power emission angle. The first term on Eqn. 1 is a normalizing factor to assure that the integral of the source radiant intensity over the entire hemisphere equals P_t . For $HPBW = 60°$, n is unity and Eqn. 1 reduces to the case of the ideal Lambertian radiator. The higher the value of n the more directive is the radiation pattern of the LED. figure 1 a) shows the LED radiation diagram using the ideal Lambertian model, $cos(\phi)$ curve, and the other curve is for a value of $n > 1$.

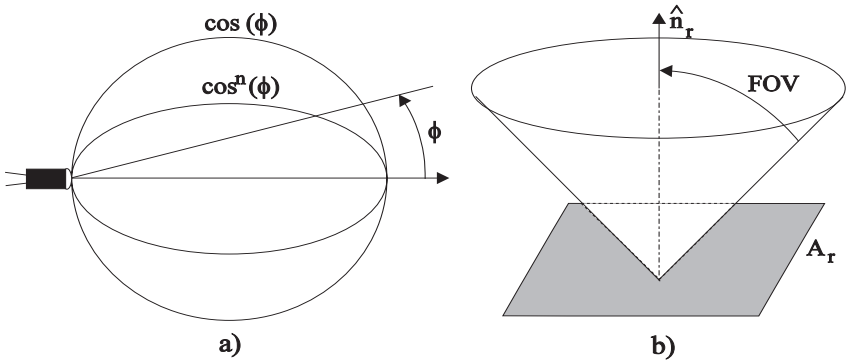

Figure 1: a) The generalized Lambertian LED model. b) The Detector Model.

3.2 The Detector Model

In indoor infrared systems, the most used detectors are large area silicon Positive-Intrinsic-Negative, PIN, photodetectors. These detectors are modelled, see figure 1 b), as having an active area, A_r, which collects the power incident for angles $\theta_i \leq FOV$.

3.3 The Channel Propagation Model

There are mainly two independent factors influencing the channel propagation characteristics: the free-space propagation losses and the signal reflections on the room surfaces. The free-space losses under consideration are described by the $1/r^2$ law. Other characteristics of atmospheric systems, like signal attenuation, dispersion and scattering, are not considered since the ranges of indoor systems are very small making those effects negligible.

The indoor infrared channel is essentially a multipath channel: if the source emits a very short pulse, like a Dirac delta function, the collected signal at the receiver will be like a "continuous" train of pulses, with different delays and amplitudes. This results from multiple reflections of the emitted pulse on all the room walls, furniture, people and any other objects.

To model the multipath dispersion effects the room reflecting surfaces are divided into incremental areas characterized by a reflection coefficient. The radiation incident on each of these areas is reflected all over the room space and the power that incides on each of the incremental areas as well as the path delay are evaluated. This model of the indoor propagation channel may be represented by a discrete low pass impulse response and can be expressed as

$$h(t) = \sum_{j=0}^{n} \sum_{k=0}^{m} a_k \delta(t - \tau_k) \tag{3}$$

where n is the maximum number of signal reflections considered on the simulation, j is the signal reflection order, k is the path index, m is the total number of paths considered for the j_{th}-reflection order, a_k represents the gain factor of

the path also called *form-factor*, τ_k represents the path propagation delay and $\delta(t)$ is the Dirac delta function. The number total of paths, m, to consider depends mainly on the room dimensions, surface characteristics and on the emitting source characteristics.

The simulation will consider the signal power that goes into the receiver after being reflected up to n times. The line of sight collected power is considered when $j = 0$, m is also zero because there is only one path to consider. The evaluation of the collected power from each order of reflection have to consider the power distribution due to the previous reflections. This distribution is a space distribution and also a time distribution due to different delays for different paths. Therefore, the a_k and τ_k have to take into account the cumulative values resulting from the signal reflections of orders lower than the one being considered.

The form-factors, a_k, in Eqn. 3 depend on the source emitting characteristics, room dimensions and on the surface reflection characteristics. The reflection characteristics of a surface depend upon the surface material and texture. To model accurately the reflection pattern found in the most common surfaces the reflection model has to be considered as a sum of two components: a non-directional or diffuse term and a directional or specular term. This is achieved by considering the reflection as a sum of two terms [4]

$$R(\theta_i, \theta_o) = R_d(\theta_i) + R_s(\theta_i, \theta_o) \tag{4}$$

where θ_i represents the incoming direction and θ_o the outgoing direction. The first term represents the signal reflected diffusely and the second term the signal reflected specularly.

An accurate evaluation of the model described on Eqn. 4 imposes very strong requirements on the computing resources. There are several simplified models describing the reflection properties of typical surfaces available from the literature [5]. The present implementation of the simulation package assumes that all incident radiation was reflected diffusely and only the first term of Eqn. 4 was considered. The reflection model reduces to

$$R(\alpha_o) = \rho \frac{1}{\pi} \cos(\alpha_o) \tag{5}$$

where ρ is the surface reflection coefficient and α_o is the angle between the outgoing direction and the surface normal. This equation represents the *Lambertian* reflection model which is characteristic of perfectly diffusing surfaces but it is also a good approximation for typical surfaces [1].

3.4 The Simulation Package

The simulation package evaluates the power distribution over all the cell area. In addition, it allows for the optimization of the power distribution through the selection of the most appropriate parameters of the emitter and receiver arrays. The optimization process has in view the reduction of the worst-case channel propagation losses. The package allows also for the simulation of the channel

impulse response. For that purpose, multiple-order reflections from the room walls have to be considered.

The input parameters of the simulation package are: the source position, orientation and emitting pattern, all the room characteristics and surface reflection properties and the receiver position, orientation and collecting characteristics. The output parameters can be the power distribution over a plane, collected power at any position, maximum channel losses, channel impulse response, etc.

4 Case Studies

The package will be used in the evaluation and minimization of the channel propagation losses for two cases corresponding to: a system with a satellite and a passive reflection based system. The optimization variable will be the emitter radiation pattern, i.e., the number, orientation and radiation pattern of the LEDs forming the optical source. The channel impulse response and the corresponding magnitude transfer function of the system with active reflection after optimization will also be presented.

4.1 System with Active Reflection

This case is representative of indoor infrared systems where the ceiling surface does not reflect the infrared radiation properly or an extension of the coverage area of the cell is required. The satellite is on the ceiling center. The stations are distributed over a plane 1 meter above the room floor. The cell is assumed circular and with a 6 m radius. The optical interfaces of the transceivers are considered to be always pointing vertically. The optimization is done for the downward link (satellite to transceiver). The main parameters of this system are presented in Table 1.

Parameter	Value
Room Dimensions ($L \times W \times H$)	$(12 \times 12 \times 4)$ m
Cell Radius	6 m
Resolution	10 cm
Satellite Position	(0, 0, 0)
Receiver Plane	(x, y, -3)
Receiver Active Area	1.0 cm^2
Receiver FOV	85°
Receiver Sensitivity	- 46.1 dBm

Table 1: - Parameters of a system with active reflection.

In the next sections, we calculate the propagation losses of a system with a satellite after the optimization process through simulation and considering all LEDs oriented in the same direction both theoretically and through simulation.

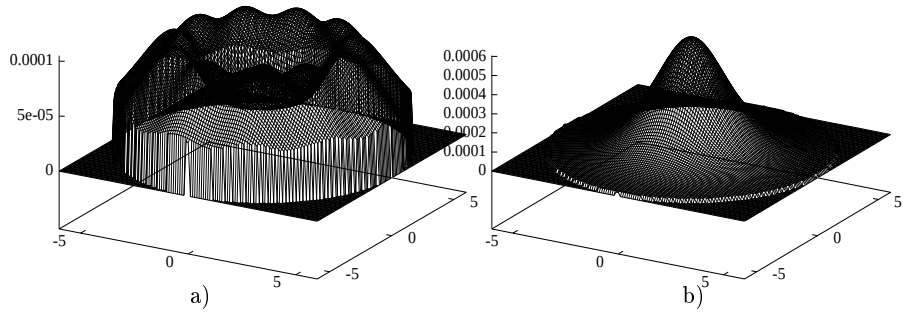

Figure 2: Irradiance profile, $[mW/cm^2]$: a) with optimization, b) without optimization.

This has in view to illustrate the gains achieved with the optimization process and to confirm the simulation package results.

4.1.1 Simulation with Optimization

After optimization, it has been found that an array of 13 commercially available LEDs emitting a total power of 152 mW would be required to illuminate this cell, assuming a receiver sensitivity of -46.1 dBm typical of a full response Manchester receiver [6]. The resulting power distribution profile after optimization is shown in figure 2 a). This power distribution was achieved by using two arrays of LEDs each with the following characteristics and orientation: 11 LEDs ($P_t = 12$ mW and $HPBW = 14°$) with an elevation angle of 62° and uniformly distributed azimuthal angles, the first LED with an azimuthal angle of 0°; 2 LEDs ($P_t = 10$ mW and $HPBW = 55°$) pointed down vertically. If LEDs with different radiation patterns were available the number of LEDs required could eventually be decreased.

According to the simulation results, the maximum channel propagation losses are 65.2 dB/cm^2 at position $(-6, 0, -3)$ and the dynamic range of the irradiance profile is 3.3 dB (maximum and minimum irradiance are -39.8 and -43.1 dBm/cm^2, respectively).

4.1.2 Theoretical Evaluation

On this evaluation, we assume that all LEDs are pointed down vertically and that all photodetectors are pointed vertically to the ceiling. The signal radiation has to cover the whole cell area, therefore LEDs with larger $HPBW$ are preferred. Thus, we consider only the LEDs with $HPBW = 55°$. Only the power that goes directly from the emitter to the receiver (line-of-sight) is considered. Under these conditions, the worst-case channel losses are at the boundary of the cell. The power collected, P_r , at the cell boundary is given by

$$P_r = \frac{n+1}{2\pi} P_t \cos^{(n+3)}(\phi_{lim}) \frac{A_r}{h^2} \tag{6}$$

where P_t and n are as defined in Eqn. 1, A_r is the detector active area and h is the height from the receiver plane to the satellite, $\phi_{lim} = \arctan(\frac{r}{h})$ and r is the cell radius. The worst-case channel propagation losses were calculated by normalizing Eqn. 6 to the total emitted power and detector active area. The losses were 68.845 dB/cm^2 at position $(6, 0, -3)$. The maximum and minimum irradiances over the cell area are -32.18 and -47.03 dBm/cm^2, respectively, giving a cell dynamic range of 14.85 dB.

4.1.3 Simulation Without Optimization

Using the simulation package, the channel propagation losses were evaluated for the system configuration presented in the last section. Figure 2 b) shows the resulting irradiance profile over the cell area.

According to the simulation results, the maximum channel propagation losses are 68.849 dB/cm^2 at position $(6, 0, -3)$. The dynamic range of the irradiance profile over the coverage cell is 14.80 dB (maximum and minimum simulated irradiances are -32.20 and -47.00 dBm/cm^2, respectively). As expected these results agree with the ones obtained through the theoretical model in last section.

By comparing the results of the optimized and non-optimized cases we verify that there was a reduction on the worst-case channel propagation losses of approximately 3.7 dB. The dynamic range of the irradiance profile was also reduced from 14.8 to 3.3 dB. These values show the significant improvement that was obtained through the optimization process.

4.1.4 Channel Impulse Response and Transfer Function

The knowledge of the channel impulse response is very important in the design of high bandwidth wireless communication systems. The simulation results of the channel impulse response of the system specified in Table 1 is shown in figure 3. The curves presented were evaluated after the optimization process and assuming the receiver at the center of the cell, dashed curve, and at the cell border, position $(5.0, 3.4, -3.0)$, continuous curve. The results show that the channel impulse response changes dramatically with the receiver position and that pulse spread due to multipath dispersion may be significant in systems for baud rates higher than a few Mbit/s. Therefore, some adaptive equalization techniques have to be considered. Due to scalling reasons, the line-of-sight received power values are not shown in the figure, those values are 79 nW and 46 nW when the receiver is at the cell center and at the cell border, respectively.

The package was also used to study the effects that each reflection order has on the channel bandwidth [7]. Figure 4 presents several curves of the channel transfer function considering up to five reflections. Each label contains the -3 dB bandwidth of the corresponding transfer function. The curve labeled "order 5" is the discrete Fourier transform of the channel impulse response shown in figure 3, continuous curve. In reference [8], the channel impulse response for several rooms was evaluated considering only reflections up to the 3rd order. Our results show that reflections at least up to the 5th order should be considered. As shown

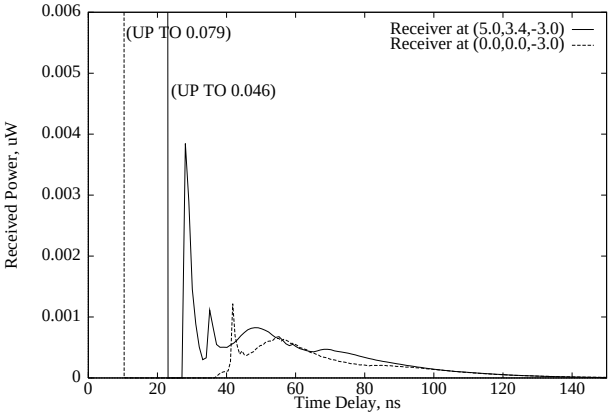

Figure 3: Channel impulse response.

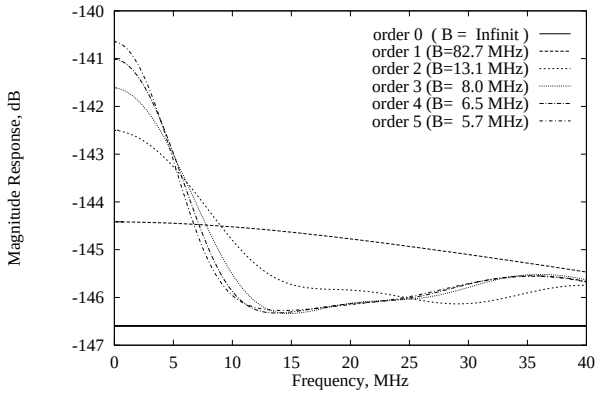

Figure 4: Channel transfer function.

in figure 4, the bandwidth considering 3 reflections is 8.0 MHz while with 5 reflections it decreases to 5.7 MHz.

The study has also shown that the optimization process reduces the variation of the line-of-sight and first order contributions with the receiver location. Moreover, it increased the channel bandwidth from 5.2 to 5.7 MHz, which is an additional benefit of optimizing the emitting pattern.

4.2 System with Passive Reflection

This case is representative of indoor infrared systems where the ceiling surface presents good reflection characteristics. The stations are distributed over the room space and have the optical interfaces pointed to the ceiling. The emitting station radiates the infrared signal towards the ceiling which is then reflected to the cell area. The main parameters of the system we will consider for simulation are presented in Table 2.

Parameter	Value
Room Dimensions ($L \times W \times H$)	$(24 \times 24 \times 4)$ m
Cell Radius	6 m
Resolution	20 cm
Ceiling Reflection Coefficient	0.8
Transceivers Plane	(x, y, -3)
Receiver Active Area	1.0 cm^2
Receiver FOV	85°
Receiver Sensitivity	- 46.1 dBm

Table 2: Parameters of a system with active reflection.

The stations are considered to be distributed over a plane 1 meter above the floor. The cell is assumed circular and placed within a large open plant (24×24) space. Thus, the reflections from the room walls can be neglected and only the reflections from the ceiling are considered. This represents a worst-case situation for the propagation losses since the reflections from the room walls would increase the power collected by the stations.

We will consider three different variants of the system specified above: non-optimized natural orientation, non-optimized targeted orientation and optimized natural orientation.

In the non-optimized natural orientation case, the transceivers are assumed to be pointed vertically. In the non-optimized targeted orientation case, the transceivers are assumed to be always pointing to the center of the cell ceiling. The results for both cases are shown in figure 5 which plots the irradiance as a function of the receiver position over the XX axis for several values of the $HPBW$. The non-optimized natural orientation case is labeled *vert* (LEDs and PINs are on the vertical) and the non-optimized targeted orientation is labeled *align* (LEDs and PINs always pointed to the ceiling center). The $HPBW$ is given by the number that follows the previous label. In the non-optimized natural orientation case the power distribution has azimuthal symmetry. In the non-optimized targeted orientation case the power distribution is not symmetric but the worst-case losses occurs in position $(6, 0, -3)$ which is shown in the figure.

Figure 5 shows that the channel losses are smaller and the irradiance over the cell area is more uniform with targeted orientation. With natural orientation the conclusion is that, the LEDs should have a wide $HPBW$. The best case, corresponds to $HPBW = 60°$ which results in a maximum channel losses of 76.6 dB/cm^2. For the same LEDs the maximum channel losses with targeted orientation decreases to 71.8 dB/cm^2. The relative reduction in the channel losses would be even higher for systems using narrower LEDs.

Targeted orientation is not very practical from the users point of view. Therefore the case of natural orientation, where the number, orientation and radiation pattern of the LEDs will be optimized in order to minimize the channel losses, will be considered. The resulting power distribution profile over the cell area is

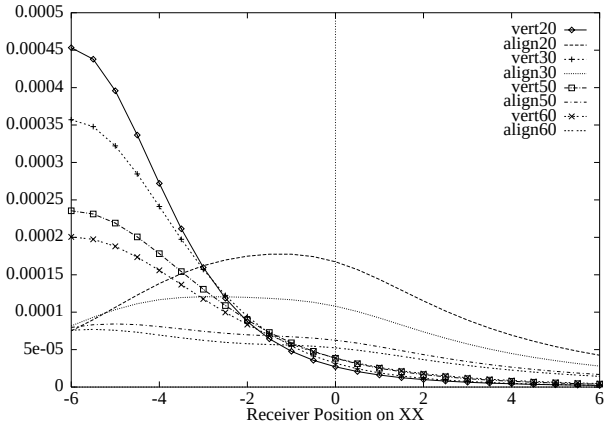

Figure 5: Power density over the cell XX axis, $[mW/cm^2]$.

shown in figure 6. This power distribution was achieved by using two arrays of LEDs with the following characteristics and orientation: 11 LEDs ($P_t = 15\ mW$ and $HPBW = 4.5°$) with an elevation angle of 72° and uniformly distributed azimuthal angles, with the first LED with an azimuthal angle of 0°; 4 LEDs ($P_t = 12\ mW$ and $HPBW = 30°$) with an elevation angle of 53° and uniformly distributed azimuthal angles, with the first LED with an azimuthal angle of 0°.

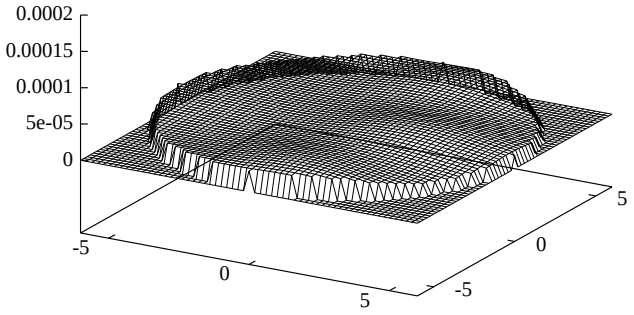

Figure 6: Irradiance profile for optimized natural orientation, $[mW/cm^2]$.

The worst-case channel losses are now 71.6 dB/cm^2. A significant reduction of 5.0 dB in the power losses relative to the non-optimized case was achieved. In addition, the worst-case channel losses are slightly lower than those obtained with targeted orientation.

Figure 7 shows the irradiance profile over the cell area for both the non-optimized cases previously discussed. As it can be seen, the optimized power distribution shown in figure 6 is significantly more uniform and the minimum irradiance is higher than on the non-optimized cases.

The channel impulse response and transfer function of the optimized system with natural orientation were simulated [7]. The results showed that passive reflection based systems present higher bandwidth than active reflection based

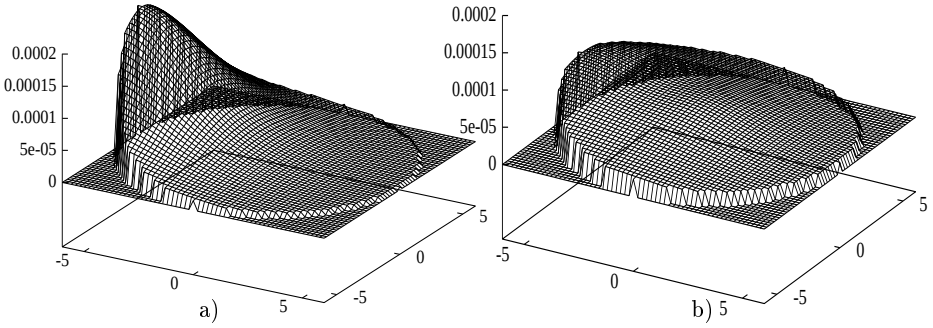

Figure 7: Irradiance profile, $[mW/cm^2]$: a) Non-optimized natural orientation. b) Non-optimized targeted orientation.

systems.

5 Conclusions

To achieve a good improvement by optimization of the power distribution profile at least two types of LEDs are required. The LEDs with narrower $HPBW$ should be pointed to the cell boundaries.

Optimization of the power distribution can reduce the worst-case channel propagation losses by several dBs and it can also reduce significantly the cell dynamic range. This improvement is comparable to that achieved by targeted orientation of the transceivers which is not very practical from the users point of view.

For the design of high performance indoor infrared communication systems with bit rates higher than a few Mbit/s the channel impulse response is very important. The results have shown that the channel impulse response changes dramatically with the receiver position. Therefore, adaptive filtering techniques have to be considered.

Optimization of the power distribution profile minimises also the changes of the line-of-sight and first-order contributions with the receiver position, reducing also the changes in the channel impulse response. In addition, it increases the channel bandwidth.

6 Acknowledgements

The first author would like to thanks JNICT - Junta Nacional de Investigação Científica e Tecnológica, for its financial support through a Ph. D. grant.

References

[1] F. R. Gfeller and U. H. Bapst. Wireless in-house data communications via diffuse infrared radiation. *Proc. IEEE*, 67(11), November 1979.

[2] K. Pahlavan. Wireless intraoffice networks. *ACM Transactions on Office Information Systems*, 6(3), July 1988.

[3] R. Valadas, A. Moreira, and A. Duarte. Hybrid (wireless infrared/coaxial) ethernet local area networks. *Proc. of the IEEE International Conference on Wireless LAN Implementation*, Sempember 1992.

[4] R. Siegel and J. R. Howell. *Thermal Radiation Heat Transfer.* Hemisphere Publishing Corp., Washington, 1981.

[5] C. R. A. Lomba. Simulation of multipath impulse dispersion on infrared communication systems. Technical report, University of Aveiro, July 1992.

[6] A. J. C. Moreira, R. Valadas, and A. Duarte. Modulation / encoding techniques for wireless infrared transmission. *IEEE 802.11 project*, (Doc. n. P802.11-93/79), May 1993.

[7] C. R. A. Lomba, R. Valadas, and A. Duarte. Update of propagation losses and impulse response of the indoor optical channel. *IEEE 802.11 project*, (Doc. n. P802.11-93/142), September 1993.

[8] J. R. Barry, J. M. Kahn, E. A. Lee, and D. G. Messerschmitt. Simulation of multipath impulse response for indoor wireless optical channels. *IEEE J. on Selected Areas in Communications*, 11(3), April 1993.